Astron. Astrophys. 324, 661–673 (1997)

ASTRONOMY
AND
ASTROPHYSICS

Carrier of the λ 5797 DIB in the ISM and in the Red Rectangle: a suprathermally rotating PAH molecule?

D. Rouan[1], **A. Léger**[2], **and P. Le Coupanec**[1]

[1] Observatoire de Paris-Meudon, Département Spatial, CNRS F-92195 Meudon Cedex, France
(e-mail: rouan@obspm.fr, lecoupanec@obspm.fr)
[2] Institut d'Astrophysique Spatiale, CNRS, bat 121, F-91405 Orsay, France (e-mail:leger@iaslab.ias.fr)

Received 10 July 1996 / Accepted 20 November 1996

Abstract. The λ5797 Diffuse Interstellar Band has recently been observed in emission at several positions in the Red Rectangle, with band shape typical of molecular rotational structures of an electronic transition. However, the rotational temperatures required to explain the observed band widths depend on the change of the rotational constant, $\Delta B/B$, of the transition but are always significantly higher than those expected for the hydrogen gas. We address the question of whether such a suprathermal rotation can be understood. Assuming that a free PAH molecule or ion is the carrier of this DIB, we investigate the physics of the rotation of such a molecule in order to interpret the observational characteristics of this emission in the RR: *(i)* a band structure indicating a rotational temperature larger than 450K at 6 arcsec from the central star; *(ii)* a decrease of this temperature with distance from the star as r^{-1}. We consider different processes of angular momentum exchange with a free PAH. We show that only an efficient rocket effect (H-atom or H_2 molecule ejection) can lead to the suprathermal rotation required by *(i)* and that its competition with radio emission can explain the power-law behaviour *(ii)*. Using observational constraints for the gas and radiation densities in the RR, we build a model and show that there is a range of molecular parameters that leads to both a good fit of the observed bandwidth and its spatial variation. Finally, we compute the bandwidth of the transition in the diffuse ISM and in Reflection Nebulae, using the same molecular parameter range. We find that they are consistent with the observed width of the λ5797 DIB in the ISM, but that the fit with RN observations narrows this range and implies a rotational constant change $\Delta B/B = -2\%$ and a PAH size of about 40 carbon atoms.

Key words: ISM: Red rectangle = HD 44179 – ISM: molecules – reflection nebulae – molecular processes

Send offprint requests to: D. Rouan

1. Introduction

Recently, a series of spectroscopic observations of the circumstellar envelope around the Red Rectangle (RR) have given a new impulse to the long standing question of the Diffuse Interstellar Bands (DIBs): for the first time DIBs *in emission* were likely evidenced (Scarrott et al., 1992). Sarre, Miles & Scarrott (1995b) have plotted the positions and widths of 3 major bands in emission as a function of the inverse of the distance to the RR central star(s). They obtained a remarkable agreement between the extrapolated curves at 1/d=0 and major DIBs in absorption (λ5797.1, λ5849.8 and λ6613.7), both for position *and* width. A chance coincidence cannot be strictly excluded, but it is our opinion that this is highly unlikely. For instance, considering the λ5797.1 plot, the extrapolation to 1/d=0 gives the position: 5997.5 $\pm$ 0.5 Åand FWHM: 1Å$\pm$ 1Å. In the interval 5790-5810 Å, there are 4 DIBs with positions (FWHM): 5789.1 (1.1), 5795.2 (4.1), 5797.1 (1.0), 5810.0 (2.6); the 2nd and 3rd one are the strongest by a factor of 4 or more (Jenniskens & Désert, 1994). The only DIB which characteristics are within the error bars ($\pm$ 1σ) is the λ5797.1 (1.0) and it is an intense band. The nearest other candidate is 5 σ away in position and 4 σ in width, pointing out the low probability of a chance coincidence. Scarrott et al., concluded to the identification of these RR emission features and to the *molecular nature* of their carriers, as the shift in position and width could be easily explained by rotational structures of the emission bands, a conclusion supported by the recent detection of a fine structure in two DIBs in absorption (Sarre et al., 1995a). Indeed, the observations of the RR emission bands revealed two specific characteristics of the features: a) a redshifted and asymmetric band profile, well explained by the rotational structure of an electronic transition with a variation of the rotational constant between initial and final electronic states, $B_{\rm f} \neq B_{\rm i}$ (Schmidt & Witt, 1991); b) a deduced rotational temperature decreasing with distance from the star as $T_{\rm rot}(r) \propto r^{-1}$ from 6 to 18 arc-sec.

The interpretation of those observations raises two questions: *i)* one can show that a change in the rotational constant

induces an observed bandwidth of $\Delta(h\nu) \propto kT_{\rm rot} \times \Delta B/B$. Since $\Delta B/B$ can hardly be larger than 3%, the data of Scarrot et al. indicate a rotational temperature in the RR larger than 450 K at 6 arc-sec of the central star. As we show in the following, this is *a temperature much larger*, by one order of magnitude, than what is expected for *the gas of the envelope*. A question is then raised: what physical processes can lead to such a high temperature? *ii)* The observed radial dependence of the rotational temperature for the DIB features in the RR is not that expected for the gas either, whatever is the gas heating mechanism that we have considered (see Sect. 3); now a new question appears: can this dependence be understood? As we will see, answering this second question is even more constraining than the first one.

In this paper we investigate the possibility that the carrier of the DIB in emission studied by Scarott et al., λ5797, is a free PAH molecule or ion. This hypothesis (van der Zwet & Allamandola, 1985; Léger, d'Hendecourt, 1985, Crawford, Tielens & Allamandola, 1985) is plausible because the carrier of this DIB is known to be a free molecule (see above) and PAHs are among the most abundant interstellar ones, possibly because they can resist the harsh UV field that illuminates the diffuse interstellar medium.

In a former paper (Rouan et al., 1992; thereafter paper I), we have studied the rotational motion of free PAH molecules, with a fixed size of $N_{\rm C}$ = 80 carbon atoms, in two different interstellar environments: a Reflection Nebula and the Diffuse Interstellar Medium. Here, in order to investigate the case of the Red Rectangle where many environmental parameters are poorly known, we propose to *extend the calculations* of Paper I to more relevant astrophysical situations. The goal of the present paper is thus two-folds: *i) to generalize the calculation of the rotational temperature* T_J to different sizes and intrinsic properties of a PAH (in Paper I we were dealing only with an average molecule of 80 carbon atoms with 1 Debye dipole moment) and to different sets of physical conditions (density, radiation field); *ii)* to investigate the consequences of the rotation in the case of a circumstellar environment, with the specific aim to model the conditions of the Red Rectangle.

The paper is organized as follows. In Sect. 2 we combine different observational constraints in order to build a self-consistent *model of the Red Rectangle* that we use to determine, or put limits on, the local conditions of radiation and density that rules the PAH rotational temperature in the envelope. In Sect. 3 we investigate the question of the *gas* temperature in the envelope around the Red Rectangle and we show that thermal equilibrium with the gas probably *cannot* explain the observed rotational temperature of the DIBs nor its dependence with distance to the central star. In Sect. 4, we establish the general formulation of the *exchange of angular momentum* for the different processes listed in Paper I, generalizing the results of this paper. We finally investigate in Sect. 5 and 6 the case of the Red Rectangle, the diffuse ISM and Reflection Nebulae (RNs), allowing variation of several parameters shows that only a restricted region in the phase space of the molecular parameters can account for the observations. The corresponding set of molecular parameters sounds plausible and gives a satisfactory fit both to the observation of the DIB in the ISM and those of Schmidt & Wittt and of Scarott et al. in the RR, providing us with valuable pieces of information on this DIB carrier.

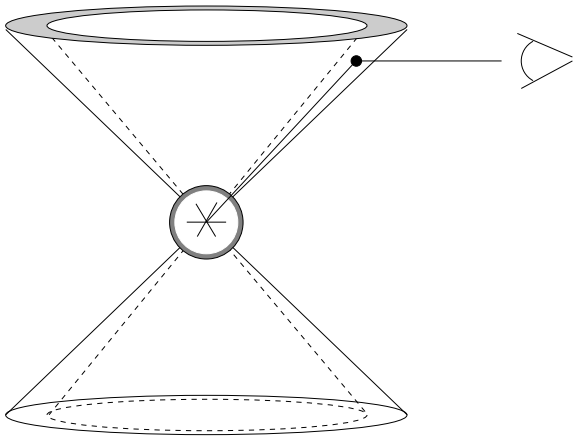

Fig. 1. Sketch of the funel geometry adopted in the model of the scattered light in the Red Rectangle

2. A self-consistent model of dust and photons in the Red Rectangle

Since several of the physical processes which constrain the exchange of angular momentum with a PAH molecule depend on the gas and radiation density, we need an evaluation of those two quantities along the whiskers of the RR where the λ5797 DIB width has been measured. The intensity of the scattered light on a given line of sight through the envelope, is directly proportional to the product of the radiation flux by the dust density, integrated along the line of sight. A simple model of the observed scattered light can thus constrain the flux density for a given gas density law, and vice-versa, if we assume a classical dust to gas mass ratio, but allow grain sizes different from those in the ISM. The model is required to explain the wavelength dependence of the scattered light. The following assumptions are made:

i) For the gas density radial distribution, we examined two cases: one that follows the classical law $n_{\rm H} \propto r^{-2}$ characteristic of a stationnary mass-loss and another one deduced from our own observations at the 3.6 m CFH Telescope in December 1993 (Rouan, Le Coupanec & Léger, 1995), using the spectrometer MOS-SIS in a long slit mode. On Fig. 2, we have plotted the intensity at 5000 Å along the NW whisker, resulting from these observations. At this wavelength, the intrinsic emission of the envelope, i.e. the fluorescence associated to the so-called Extended Red Emission, is negligible and it is essentially the light scattered on grains which is seen. Its intensity follows a $r^{-2.6}$ power-law in the range of angular radius studied. If the envelope is optically thin on the line of sight, one shows that this law would be characteristic of a density varying as $n_{\rm H} \propto r^{-1.6}$.

ii) For the central exciting star, two cases have been examined: a 10 000 K B9-A1 (Cohen et al., 1975) and a 7500 K star, as derived more recently from spectroscopic observations by

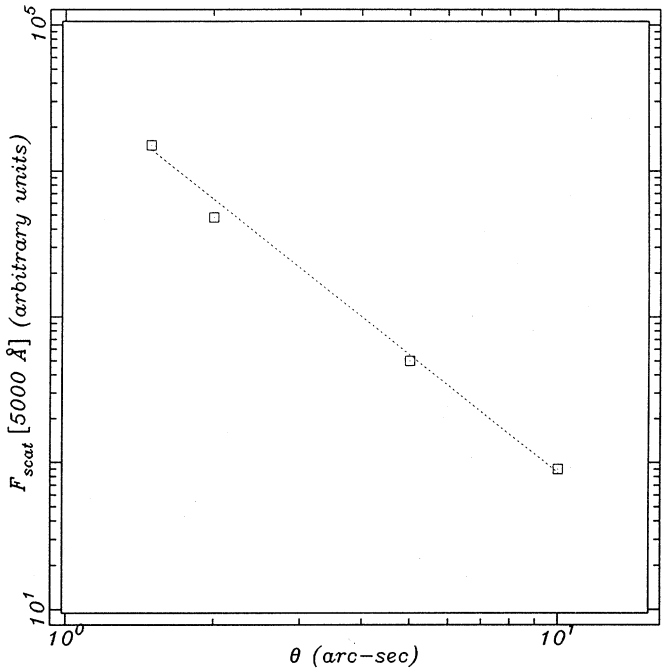

Fig. 2. Radial variation of the scattered light intensity at 5000 Å, along the NW whisker of the Red Rectangle nebula. The data were obtained at CFHT, using the MOS-SIS spectrograph in Nov 1993. The log-log scale shows that a power-law of index -2.62 gives a good fit.

Waelkens et al. (1992). We cannot exclude that there is a hidden companion star to HD44179, that would actually be at the origin of the bipolar outflow, as suggested by several observations (Waelkens et al., 1996; Van Winckel et al., 1995, Roddier et al., 1995, Tessier et al., 1990); this might be what makes the RR so specific. In any case, since the spectral properties of the light illuminating the whiskers are derived from the scattered part of the spectrum on which emission features are observed (see *vi)* hereafter), we can safely assume that there is no extra illumination that we would miss.

iii) A Kurucz model (1979) is used for the *spectrum* of the stellar light injected in the envelope. We prefer using a synthetic model for the photospheric emission of the star rather than the measured one, because any measured spectrum, even in a small diaphragm centered on the peak brightness of the nebula, will necessarily be affected by circumstellar matter absorption and contain an additional component of scattered light that cannot be disentangled from the pure stellar emission.

iv) As we want to consider only scattered light, we have taken into account only the 3400 Å– 4200 Å range to avoid the Extended Red Emission (ERE) that becomes dominant beyond 5000 Å(Warren-Smith, Scarrott & Murdin, 1981).

v) The *grain model* is a mixture of graphite and silicate (Draine & Lee, 1984), with $n(a) \propto a^{-3.5}$ (MRN distribution), but with $a_{\max}$ left as a free parameter. Note that one could consider a model with only carbon grains, since it is generally admitted that the RR is a C-rich envelope (strong 3.3 μm feature), but this would hardly change the conclusion because the optical properties at those wavelengths are essentially dominated by the *carbon component*.

vi) Concerning the *structure of the envelope*, as in the model of Yuseph-Zadeh, Morris & White (1984) and of Lopez, Mékarnia & Lefèvre (1995), we assume that the *matter is essentially concentrated in a funnel*, and that there is a *void bicone* along the main axis (South-North), so that the whiskers are nothing but the wall of the cone scattering the light that propagates easily in the funnel. Fig. 1 sketches the geometry of the model. In order to explain the colour of the scattered light which is redder than expected from an unreddened 7500 K star, we assume that an extinction occurs very close to the star in a thin shell; the rest of the biconical envelope, i.e. the region extending beyond, say, one arcsec, which is accessible to observation, is supposed optically thin: we will see *a posteriori* that this hypothesis is not fully justified, but should not change drastically the conclusion. We do not try to derive the extinction in the inner shell directly from photometric measurements on the star because it can be different towards the observer – where a disk is probably present – and towards the biconical nebula. We derive it from the colour properties of the scattered light as follows.

Mie computation of $< Q_{\rm ext} >$ and $< \phi(\theta) \times Q_{\rm sca} >$ is performed, where $\phi(\theta)$ is the phase function of scattering ; the bracket symbol means that the average is done on a MRN distribution. The extinction of the light in the inner shell is given by $exp(-C\langle Q_{\rm ext}\rangle)$, where C is a quantity proportional to the gas column density; the intensity of the light scattered towards the observer is proportional to $\langle \phi(\theta) \times Q_{\rm sca}\rangle$, where θ is the scattering angle. For the sake of simplicity, we assume that all photons have suffered a scattering at right angle (θ = 90 deg), because, on a given line of sight, most of the scattered photons come from the points closest to the star where both the highest dust density and the highest incident radiation are found.

With these hypotheses, at a given wavelength, the expression of the ratio of scattered to intrinsic stellar light is:

$$R = F_{\rm Neb}/F_* \propto \langle \phi(\theta = 90\,{\rm deg}) \times Q_{\rm sca}\rangle \; exp(-C\langle Q_{\rm ext}\rangle)$$

The ratio $R(\lambda_1)/R(\lambda_2)$ depends only on the stellar spectrum and on the grain optical properties, but not on structural parameters such as the density. Since brightness measurements of the scattered light are available at different wavelengths (Warren-Smith et al., 1981), we look for the dust model that gives the best fit of the observations: $a_{\max}$ is adjusted so that a single value of C can be found for all wavelengths between 3800 and 4300 Å; then, the value of the optical depth in the shell is derived:

$$\tau_{\rm ext} = C\langle Q_{\rm ext}\rangle$$

For a star with an effective temperature $T_{\rm eff}$ = 7500K, the best fit is found for $a_{\max}$ ranging from 0.05 to 0.1 μm, implying $\tau_{\rm ext}(V)$ = 1.26, a value consistent with the bolometric to visible stellar flux ratio that requires $A_{\rm V} < 2.7$. For a star with an effective temperature T_* = 10000K, the derived extinction is too large, and we have therefore rejected this case. One notes that, within this range of $a_{\max}$, $\tau_{\rm ext}$ remains almost constant: the model is *not* sensitive to the exact value of $a_{\max}$.

Since $\tau_{\rm ext}$ and $Q_{\rm sca}$ are now constrained, we can estimate the ratio $R = F_{\rm Neb}/F_*$. With the hypothesis of an optically thin line of sight, one can show that the expression of R reads:

$$R = 6.03\ 10^{-4} D\ \sigma_s(\alpha^2/\theta) n_{\rm H} m_H G_1 exp(-\tau_{\rm ext}) = 3.0\ 10^{-6}\ (D/1{\rm kpc})\ \sigma_s(\alpha^2/\theta) n_{\rm H} G_1 exp(-\tau_{\rm ext}) \quad (1)$$

where σ_s is the equivalent scattering cross section of grains per unit mass, is expressed in cm^{2}g^{-1} and $n_{\rm H}$ in cm^{-3}. D is the distance of the Red Rectangle, α *is the angular size of the diaphragm in which the scattered light is measured*, θ is the angular distance from the star to the point where scattering light is measured and G_1 is a dimensionless geometric factor depending on the conical structure of the envelope, whith value close to 1. Note that the canonical ISM value of 100 was taken for the ratio of gas to dust masses.

The above expression of $R(\lambda)$ fits the observations in the whole range 3800–4300 Å.

In the expression of the ratio $R = F_{\rm Neb}/F_*$, F_* refers to the intrinsic flux from the star, the one that would be measured if there were no extinction between the observer and the star. To evaluate this flux, we use the star's bolometric flux, 3.0 10^{-7} ergcm^{-2}s^{-1}, from Schmidt et al (1980) and the model of stellar atmosphere from Kurucz (1979). One finds F_* = 5.97 10^{-10} erg cm^{-2}s^{-1} nm^{-1} at λ = 5000 Å, for a star of effective temperature $T_{\rm eff}$ = 7500 K.

Concerning the scattered light, we used the data on Fig. 1 of Schmidt et al. (1980). Using information from their paper, the ratio of visible to bolometric flux is $F_{\rm vis}/F_{\rm bol} = 1/12$ and at 5000 Å, the ratio of fluxes measured in two diaphragms, one at 10 arcsec from the star and one on the star itself is 1/1300, one finds $F_{\rm Neb}$ = 5.24 10^{-14} erg cm^{-2} s^{-1}nm^{-1}.

Observational data lead then to R = 8.78 10^{-5}. We can now derive $n_{\rm H}(\theta$ = 10") from Equ.1:

$$n_{\rm H}(\theta = 10") = 2.34\ 10^3 exp(1.12\tau_V)(D/1{\rm kpc})^{-1}\ {\rm cm}^{-3}$$

On the other hand, the radiation density in the envelope is given by:

$$U_\lambda(r) = L_*(\lambda)\exp(-\tau_\lambda)/(4\pi\ c\ r^2)$$

where the λ dependence of $L_*(\lambda)$ is given by the Kurucz model for T_* = 7500 K and that of τ_λ by our grain model scaled with τ_V = 1.26. Taking into account the visible-UV cross-section, $\chi(\lambda)$, of a typical PAH, measured by Joblin et al. (1992), we are now able to compute the number of UV photons absorbed per unit of time by a given PAH:

$$n_{\rm UV} = \int U_\lambda(r) h^{-1} \chi(\lambda) \lambda d\lambda, \quad h \text{ being the Planck constant.}$$

To summarize, the *characteristic parameters of the RR whisker* that we will use in the model are:

$$U_{\rm UV}(\theta) = 4.0(\theta/10'')^{-2}\ {\rm eV\ cm}^{-3}$$
$$n_{\rm H}(\theta) = 1.6\ 10^4\ (D/1{\rm kpc})^{-1}\ (\theta/10'')^{-1.6}\ {\rm cm}^{-3}$$
$$T_* = 7500\ {\rm K}$$
$$T_{\rm gas} = 35\ {\rm K}$$
$$A_V = 1.7$$

where $U_{\rm UV}$, given in eV cm^{-3} is the integral of U_λ over the wavelength range where PAHs absorb.

3. Kinetic temperature of the circumstellar gas in the Red Rectangle

The first natural idea to explain the observed PAH rotational temperature in the RR is that the molecule is in collisional equilibrium with the gas, this one being hot, and its temperature decreasing with the distance to the star simply because of the dilution of radiation. To test the validity of this hypothesis, we consider the two classical mechanisms for the gas heating: collisions with the grains and photo-electric effect on aromatic molecules. Our two criteria to check the validity of the process are: the absolute value of the temperature obtained, say at 10 $''$, and its dependence upon the distance to the star.

3.1. Heating by collisions with grains

Grains in the envelope can be efficiently heated by the photospheric emission of the central star and, in turn, can become a source of energy to heat the gas by collision. However, a well established fact is that the thermalization on grains can be effective only when the gas density is quite large: in other words, the gas temperature is much below the grain temperature ($T_{\rm g} \ll T_{\rm d}$) as long as $n_{\rm H} < 10^{6-8}$ cm^{-3} (e.g. Spitzer, 1978). This is because the cooling of the gas in the far-infrared through emission in C$^+$ lines is very efficient as long as the optical thickness of the cloud at those wavelengths is below unity. The equation of equilibrium between C$^+$ cooling and grain heating, when the gas density is below say 10^6 cm^{-3} (we have seen in Sect. 2 that the density at 10 $''$ is in the range $10^4 - 10^5$ cm^{-3}), reads, in CGS units, (Spitzer, 1978):

$$7.9\ 10^{-27}\ n_{\rm H}^2\ d_C\ \exp(-92K/T) = 1.35\ 10^{-33}\ (\frac{a}{0.1\mu m})^{-1}\ (\frac{\rho_{\rm d}}{2\ g\ {\rm cm}^{-3}})^{-1}\ n_{\rm H}^2\ T^{1/2}\ (T_{\rm d} - T)$$

where a, $T_{\rm d}$ and $\rho_{\rm d}$ are respectively the radius, temperature and mass density of the dust grain; d_C is a coefficient expressing the efficiency of the cooling through C$^+$. Solving this equation gives a gas temperature which is always below 20 K, even for grains as hot as 10000K, as long as $n_{\rm H} < 10^{6-8}$ cm^{-3}. On the other hand, the maximum grain temperature one can expect at a given location in the envelope of the RR would be for zero extinction and low-emissivity (e.g. graphite) grains: those conditions lead to $T_{\rm Graphite}$ = 110 K at $\theta = 10''$. Then, if only heated by grains, the gas temperature would be $\approx$ 10 K at $\theta = 10''$.

Second, we note that, if we assume $Q_{\rm abs} \propto \lambda^{-1}$ and, as strongly suggested by observation (Sect. 2), that extinction in the nebula, along a radial path towards outside, becomes negligible beyond, say, the first arcsec, then $T_{\rm d} \propto r^{-2/5}$, a behaviour which

is quite different from the much steeper r^{-1} law observed in the RR by Scarott et al.

3.2. Photo-electric effect

Because of the low ionization potential of PAHs, electrons are easily extracted from those abundant IS molecules by UV photons, and have a kinetic energy that can efficiently heat the gas (d'Hendecourt & Léger, 1987). Using the evaluation by those authors of the photo-electric heating rate, and balancing it with the cooling through C^+ infrared lines, one obtains:

$$7.9\ 10^{-27}\ n_{\rm H}^2\ d_C\ \exp(-92K/T) = f[\frac{C}{H}]n_{\rm H}(1-\beta)\frac{Q_o}{N_{\rm C}}, \quad (2)$$

where f is the fraction of cosmic carbon in PAHs, β the fraction of ionized PAHs and $Q_o/N_{\rm C}$ the heating rate per carbon atom in the molecule which is proportional to the UV density. Note that, if $n_{\rm H}$ varies as r^{-2} in the gas envelope of the Red Rectangle, as one expects in a steady-state mass loss, and $U_{\rm UV}$ as r^{-2} because of the geometrical dilution of radiation (no extinction in the upper part of the nebula), then both sides of the equation contain a r^{-4} dependence that cancel out. The gas temperature would then be *independent of the distance to the star*. To calculate this temperature, we have first to know the degree of ionisation, β, of PAH molecules. Using the evaluation of the ionization and recombination rates $R_{\rm ion}$ and $R_{\rm rec}$ from d'Hendecourt & Léger (1987), and scaling them to the UV flux ($U_{\rm UV}$), electron temperature (T_e) and gas density in the RR (see 2), we find:

$$\begin{aligned}\beta &= \frac{R_{\rm ion}}{R_{\rm ion}+R_{\rm rec}}\\ &= \frac{9.65\ 10^8(U_{\rm uv}/.08{\rm eV})}{9.65\ 10^8(U_{\rm UV}/.08{\rm eV})\ +\ 2.9\ 10^9(T_e/80)^{1/2}(n_{\rm H}/10)}\\ &= .016\end{aligned}$$

The PAH are thus almost totally neutral ($\beta \approx 0$). To evaluate the temperature from Equ. 2, we use $f = 0.15$, $[\frac{C}{H}] = 4\ 10^{-4}$ and the evaluation done by d'Hendecourt & Léger for $Q_o/N_{\rm C}$ in the Interstellar Radiation Field, scaling it to the case of the Red Rectangle ($U_{\rm UV} = 4(\theta/10'')^{-2}$eV cm^{-3}, see Sect. 2); this leads to $\exp(-92/T) = 7.1\ 10^{-3}$, or $T = 35$ K, independent of θ.

A strong conclusion is thus that, if we assume classical heating mechanisms, *the gas temperature i) should be much lower than the observed DIB rotational temperature and ii) does not follow the r^{-1} law*.

An independent evaluation that supports this conclusion is obtained by simply scaling the gas temperature in IRC+10216, estimated or measured by other authors (Keady, Hall & Ridgway, 1984), to the situation of the RR. Taking into account the differences in distances and luminosities of the central stars in both objects, we find $T_{\rm d} = 50$ K and $T_{\rm g} = 10$ K at a radius corresponding to $\theta = 10''$ in the RR. This is consistent with our estimate of the gas temperature.

One cannot exclude that the gas is heated by another mechanism, specific of the mass-loss process (compression in shocks that would be regularly distributed in the whole nebula?) - measurements of the actual gas temperature in the Red Rectangle by any technique would be extremely useful - however we assume in the following that this is not the case and we use a gas temperature of 30 K and look for a more efficient way to heat the rotational motion of the molecule responsible for the λ 5797 DIB.

4. Rotational temperature T_J of a PAH molecule

In Paper I, we have computed the rotational temperature of a 90 atoms PAH molecule considered as the "average" aromatic molecule found in the ISM. In the same paper (Sect. 9) we computed the rotational temperature of a classical grain, i.e. a non-planar particle, versus its size. The processes that exchange angular momentum with the molecule and that we took into account are:

- collisions with the gas: elastic or inelastic when a H-atom binds to the molecule, with subsequent:
- ejection of H or H_2 species, for instance as a consequence of a UV photon absorption; a peculiar and important case is an asymmetric ejection that leads to a systematic rocket effect
- absorption of UV photons
- emission of IR photons after such an absorption
- emission of radio rotational photons

The main results of Paper I can be summarized as follows:

- The angular momentum of an interstellar PAH with $N_{\rm at} = 90$ ($\approx$ 78 C atoms) is mainly built-up by the emission of IR rovibrational photons, through a random walk ($\Delta J = \pm 1$) with an asymmetric probability.
- The resulting distribution of J, is pseudo-thermal with $kT_J = h\nu_o/6$, where $\lambda_o = c/\nu_o$ is the average wavelength of the IR photons emitted during the cooling phase that follows the absorption of a UV photon. Typically, $T_J \approx$ 120K for a molecule with 90 atoms.
- The Interval Vibrational Rotational Energy Transfer (IVRET, Mc Clelland et al., 1988) is an extremely efficient mechanism that forces the large inertia axis of the molecule to be distributed around the angular momentum $\boldsymbol{J}$ with the same temperature as the vibrations (for a symmetric top molecule, $T_K = T_{\rm vib}$). This axis is either almost isotropically distributed and suffers frequent changes just after the absorption of a UV photon ($T_{\rm vib} >> T_J$) or aligned along $\boldsymbol{J}$ during the cold periods in between thermal spikes ($T_{\rm vib} << T_J$).
- Collisions with the gas are marginally significant even for densities typical of Reflection Nebulae

In this section we propose to extend the analysis done for a planar PAH, from 78 carbon atoms to *other sizes*, using as a guideline Paper I - Sect. 9.

The construction of J can be considered as a random walk in a potential well with a minimum at $J = \bar{J}$ where the net systematic rate of change of J is zero:

$$(\sum_i \tau_i^{-1} \Delta J)_{\bar{J}} = 0,$$

where τ_i is a characteristic time between two events of process i. ΔJ has two components: (1) $\Delta_1 J$ generated by the asymmetry of the process, e.g. that due to the ν^3 dependence of the Einstein coefficient of spontaneous emission; (2) $\Delta_2 J$ generated by the random walk itself and estimated as follows. At each event, $\boldsymbol{J}$ becomes $\boldsymbol{J} + \boldsymbol{\delta J}$, with $\boldsymbol{\delta J}$ randomly oriented; after N events, without systematic effect, the mean modulus would be $J = N^{1/2}\ \delta J$; the mean increase per event is then: $\Delta_2 J = \frac{1}{2}\ (\delta J)^2/J$. [1] The resulting distribution of J has its maximum at $\bar{J}$. In the following, we will thus establish the quantities $\tau_i^{-1}\Delta J$ for each process that exchanges angular momentum with the molecule.

4.1. Contribution of IR emitted photons

A burst of emission of IR photons follows, during a few seconds, the transient heating by absorption of a UV photon by a PAH. The change of angular momentum is then $\pm\hbar$ per IR photon, or $\delta J = \pm 1$.

The asymmetry terms in the J change per emitted IR photon are (Paper I Sect. 9.1 and above remark):

$$\Delta_1 J_{\rm IR} = -\frac{1}{J_{\rm IR}}(\frac{J}{J_{\rm IR}} - \frac{J_{\rm IR}}{J})$$

$$\Delta_2 J_{\rm IR} = \frac{1}{2J},$$

with $J_{\rm IR} = (kT_{\rm J}/B)^{1/2}$, where B is the rotational constant and $1.5 \times T_{\rm J}$ the rotational temperature when emission of IR photons is the dominant mechanism for building the angular momentum.

We establish now the dependence of B and T_J upon $N_{\rm at}$.

For a planar particle with the same density as graphite, the relationship between its number of atoms $N_{\rm at}$, radius a and geometrical surface S are: $N_{\rm at} \propto a^2$ and $S \propto N_{\rm at}$, thus $B \propto (M\ a^2)^{-1} \propto N_{\rm at}^{-2}$.

We have shown (Paper I) that $kT_J = h\nu_o/6$ where ν_o is the average frequency of emitted IR photons, defined as

$$\nu_o^{-1} = \frac{1}{N} \sum_j n_j \nu_j^{-1}\ ,$$

or $\lambda_o = < \lambda >$; this expression put weights on long wavelength photons which are emitted when the molecule temperature is rather low. Therefore, we use a simple model for "large" molecules, valid at low temperature ($T < \theta_D$, when θ_D is the Debye temperature): *i)* the long wavelength emissivity of the molecule is continuous and $Q_{\rm abs}(\lambda) \propto \lambda^{-1}$ (Léger, d'Hendecourt and Défourneau, 1989); *ii)* the heat capacity is $C(T) \propto T^2$.

The average wavelength of the emitted photons at a given temperature T is, with the above assumptions:

$$\lambda_T = \frac{\int B_\lambda Q_{\rm abs}(\lambda)\lambda d\lambda}{\int B_\lambda Q_{\rm abs}(\lambda) d\lambda} = (T/5280\ {\rm K})^{-1}\ \mu{\rm m}$$

During the period of time where the molecule cools by dT, the number of "average" photons emitted is:

$$dN = C(T)/h\nu_o\ dT \propto T\ dT$$

The mean wavelength of photons emitted during the complete cooling is:

$$< \lambda_T > = \frac{\int \lambda_T dN}{\int dN} = \frac{\int_0^{T_{\rm peak}} dT}{\int_0^{T_{\rm peak}} (T/5280\ {\rm K})\ dT}$$
$$= (T_{\rm peak}/10560)^{-1}\ \mu{\rm m} \qquad (3)$$

We derive $T_J = hc\ (6k < \lambda_o >)^{-1} = 0.23\ T_{\rm peak}$ for large molecules ($N_{\rm at} > 100$).

Now, the behaviour of $T_{\rm peak}$ with $N_{\rm at}$ is ruled by the heat capacity law and the energy E_{UV} of the absorbed UV photon:

$$E_{\rm UV} = \int_0^{T_{\rm peak}} C(T) dT\ ,$$

or

$$T_{\rm peak}\ N_{\rm at}^{-1/3}$$

Combining the previous relations leads to:

$$J_{\rm IR} = (\frac{kT_J}{B})^{1/2} \propto (\frac{N_{\rm at}^{-1/3}}{N_{\rm at}^{-2}})^{1/2} \propto N_{\rm at}^{5/6}\ .$$

Taking into account the proper emissivity and heat capacity, one can show that this relation holds within a factor 2 even for small PAH.

The variation in J per IR photon emitted is:

$$(\Delta J)_{\rm IR} = -\frac{1}{J_{\rm IR}}(\frac{J}{J_{\rm IR}} - \frac{3}{2}\frac{J_{\rm IR}}{J})$$

with $J_{\rm IR} = 270\ (N_{\rm c}/78)^{5/6}$ where the normalisation has been done relatively to the 90 atoms (78 carbons) molecule of Paper I.

The rate of IR photons emission, $\tau_{\rm IR}^{-1}$, varies with the size of the molecule because of the increase of its UV cross section and because the average wavelength of IR photons changes with peak temperature:

$$\tau_{\rm IR}^{-1} = \tau_{\rm UV}^{-1} \frac{\lambda_{\rm IR}}{\lambda_{\rm UV}},$$

with $\tau_{\rm UV}^{-1} \propto N_{\rm at}$ and $\lambda_{\rm IR} \propto T_{\rm peak}^{-1} \propto N_{\rm at}^{1/3}$, or:

$$\tau_{\rm IR}^{-1} = 10^{-2}(\frac{N_{\rm C}}{78})^{4/3},$$

[1] Note that the term $\Delta_2 J$ *was uncorrectly omitted in Paper I*

and:

$$(\tau^{-1}\Delta J)_{\rm IR} \;=\; -3.7\ 10^{-5}\ [\frac{J}{270}(\frac{N_{\rm C}}{78})^{-1/3} - \frac{3}{2}\frac{270}{J}(\frac{N_{\rm C}}{78})^{4/3}]\ s^{-1}.$$

This last equation shows that the process is self-regulating, and would lead, if alone, to the value $J = 1.22 J_{\rm IR}$ at equilibrium. One must note that the pull-back effect to $J = 1.22 J_{\rm IR}$ is tight (see Fig. 3 of Paper I) and will *clamp the rotational temperature to* $T_{\rm IR} \approx 100K$ *if the UV density is high enough* .

4.2. Contribution of H_2 ejection

We assume that the ejection of hydrogen is mostly molecular (H_2) (Paper I, Sect. 4.2.2). The associated "rocket effect" exists only if there are hetero-atoms or pentagonal cycles (Paper I, Sect. 4). We assume that the systematic orientation of this ejection versus its random one can be described by a parameter $\alpha_{\rm asym}$ giving the ratio of hydrogen ejections that produce a systematic torque to those with a mean zero torque, when averaged over a large number of events. We assume in addition that $\alpha_{\rm asym}$ does not depend on the size of the PAH (typically one can expect $\alpha_{\rm asym} \leq 0.1$). The resulting change of J is dominated by $(\Delta_1 J)_{\rm rocket}$ whenever $\alpha_{\rm asym} \neq 0$, or:

$$(\Delta J)_{\rm rocket} \;=\; -J m_H a^2/I + \alpha_{\rm asym}(m_H a^2 E_{\rm ej})^{1/2}$$

where the first term corresponds to the friction due to sticking H-atoms, and the second one to the systematic rocket effect. Taking into account the dependence upon $N_{\rm at}$ of I and a reads:

$$(\Delta J)_{\rm rocket} \;=\; -(N_{\rm C}/78)^{-1} J/250 + 2 \times (N_{\rm C}/78)^{1/2}$$

On the other hand, the rate of ejection of H_2, half the rate of collisions with H atoms, is:

$$\begin{aligned}
\tau_{\rm ej}^{-1} \;&=\; n_{\rm H} v_H \pi a^2 \\
&=\; 1.66\ 10^{-6}(N_{\rm C}/78)(n_{\rm H}/10^3{\rm cm}^{-3}) \\
&\quad\times(T_{\rm g}/100\ {\rm K})^{1/2}(\beta/.98)\ \ {\rm s}^{-1},\ \ \text{and} \\
(\tau^{-1}\Delta J)_{\rm rocket} \;&=\; 1.66\ 10^{-6}[-J/250\ + 2(N_{\rm C}/78)^{3/2} \\
&\quad\times(\alpha_{\rm asym}/0.1)(E_{\rm ej}/0.1\ {\rm eV})^{1/2} \\
&\quad\times(T_{\rm g}/100\ {\rm K})^{1/2}(\beta/.98)\ \ {\rm s}^{-1}
\end{aligned}$$

4.3. Radio rotational photons

If the molecule has a non-vanishing static dipole moment μ, its rotation generates spontaneous emitted radio photons. A likely possibility for $\mu \neq 0$ is the presence of hetero-atoms in an aromatic molecule.

We admit that the radio emission power of a PAH molecule is of the same order of magnitude as that of a linear species with the same electric dipole and a rotational constant equal to that around the disk main axis ($C = B/2$). Such an emission corresponds to a systematic decrease of J, $\Delta J = -1$, with a probability given by the Einstein coefficient $A_{J\rightarrow J-1}$. For $J >> 1$, and using $h\nu = 2CJ$, this coefficient is (Herzberg, 1968; Townes and Schawlow 1975):

$$A_{J\rightarrow J-1} = \frac{256\pi^4}{3h^4c^3} B^3\mu^2(1+\frac{1}{2J})^{-1}J^3,$$

Since $B \;\propto\; N_{\rm at}^{-2}$, there is, for a given μ, an extremely fast dependence of $A_{J\rightarrow J-1}$ with the molecule size:

$$A_{J\rightarrow J-1} \;\propto\; N_{\rm C}^{-6}\ \mu^2\ J^3$$

This will drastically limit rotational temperature of small particles because they will cool very efficiently by radio emission. Unlike in Paper I, the contribution of emitted radio rotational photons cannot be neglected in the building-up of J, since we do not exclude here that small molecules can be responsible of the observed DIB.

4.4. Resulting most probable J and rotational temperature

The budget of the different contributions, that determines the most probable J, noted $\bar{J}$, is, when including elastic collisions:

$$(\tau^{-1}\Delta J)_{\rm IR} + (\tau^{-1}\Delta J)_{\rm rocket} + (\tau^{-1}\Delta J)_{\rm radio} + (\tau^{-1}\Delta J)_{\rm coll} \;= 0,$$

where the subscript coll designates elastic collisions only, the inelastic ones are included in the term describing the rocket effect. This equation reduces to:

$$-\,a_{\rm radio}J^3 - (b_{\rm IR} + b_{\rm friction})J + c_{\rm rocket} + (d_{\rm IR} + d_{\rm coll})J^{-1} = 0 \quad (4)$$

with:

$$\begin{aligned}
a_{\rm radio} \;&=\; 1.9\ 10^{-15}\ (\frac{N_{\rm C}}{78})^{-6}\ (\frac{\mu}{1{\rm Debye}})^2, \\
b_{\rm IR} \;&=\; 3\ 10^{-7}\ (\frac{N_{\rm C}}{78})^{-1/3}\ (\frac{U_{\rm UV}}{50\ {\rm eV\ cm}^{-3}}), \\
b_{\rm friction} \;&=\; 1.8\ 10^{-9}\ (\frac{n_{\rm H}}{10^3\ {\rm cm}^{-3}})\ (\frac{T_{\rm g}}{100{\rm K}})^{1/2}, \\
c_{\rm rocket} \;&=\; 1.8\ 10^{-6}\ (\frac{N_{\rm C}}{78})^{3/2}\ (\frac{n_{\rm H}}{10^3\ {\rm cm}^{-3}})\ (\frac{T_{\rm g}}{100\ {\rm K}})^{1/2} \\
&\quad\times(\frac{\alpha_{\rm asym}}{0.1})\ (\frac{E_{\rm ej}}{0.1{\rm eV}})^{1/2}\ \delta, \\
d_{\rm IR} \;&=\; 3\ 10^{-2}\ (\frac{N_{\rm C}}{78})^{4/3}\ (\frac{U_{\rm UV}}{50\ {\rm eV\ cm}^{-3}}), \\
d_{\rm coll} \;&=\; 6.8\ 10^{-4}\ (\frac{N_{\rm C}}{78})^2\ (\frac{n_{\rm H}}{10^3{\rm cm}^{-3}})\ [\frac{2}{3}\ (\frac{T_{\rm g}}{100{\rm K}})^{1/2} \\
&\quad\times(\frac{E_{\rm ej}}{0.1{\rm eV}})\ \beta\ \delta\ +\ \frac{1}{3}\ (\frac{T_{\rm g}}{100{\rm K}})^{3/2}\ (1-\beta)],
\end{aligned}$$

Where β and δ are the ionization and deshydrogenation fractions of the PAH.

We show in Appendix A that this equation has a unique positive real solution.

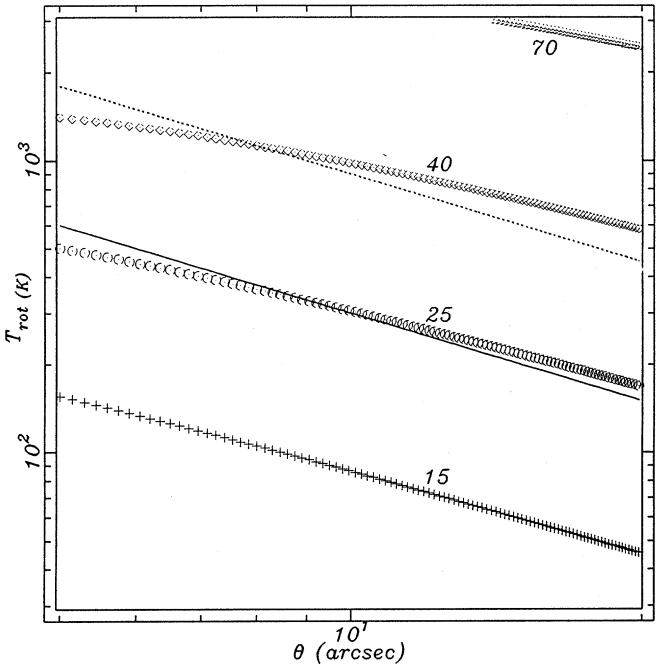

Fig. 3. Rotational temperature of a PAH molecule in the Red Rectangle, as a function of the angular distance to the central star. The solid and dotted lines are the observed $\approx r^{-1}$ law, when assuming $\Delta B/B$ = 3% and 1%, respectively. The other curves correspond to the temperatures calculated with our model, for different sizes of the PAH, they are labelled with the number of carbons. The set of parameters is: $\alpha_{\rm asym}\ E_{\rm ej}^{1/2}$ = .3eV$^{1/2}$, $A_{\rm V}$ = 2.0, $T_{\rm g}$ = 10$(\frac{\theta}{10''})^{-.7}$ K, μ = 3.0 Debye. We note a reasonable agreement between observed and theoretical data for PAH from 25 carbons ($\Delta B/B$ = 3%) to 40 carbons ($\Delta B/B$ = 1%).

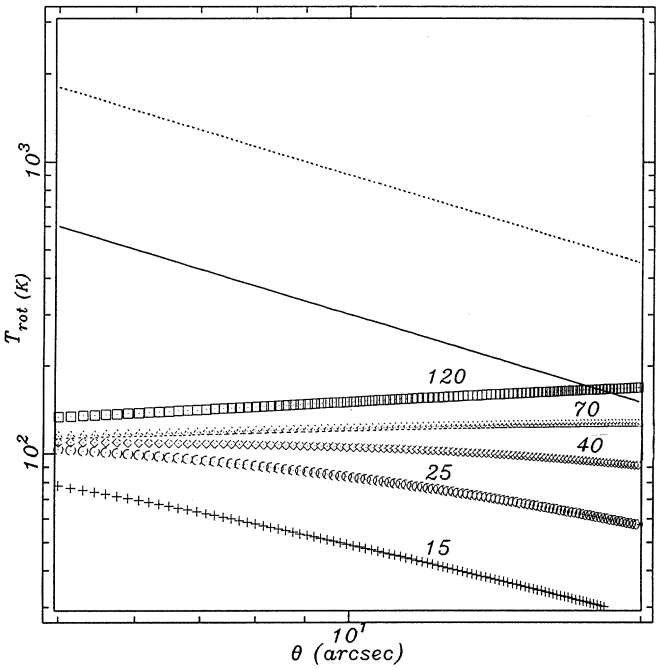

Fig. 4. Same as Fig. 3, but with $\alpha_{\rm asym}\ E_{\rm ej}^{1/2}$ = .03 eV$^{1/2}$: there is no acceptable fit of the slope wathever the PAH size is.

5. Rotational temperature in the Red Rectangle

Taking into account the parameters evaluated in Sect. 2, we solve now Eq. 4 in the case of the Red Rectangle.

In the following, we compare the observed radial dependence of the rotational temperature deduced from Scarrott et al. (1992) to the one found with our model. We plot the temperature for different sizes of PAH particles ranging from 15 to 120 carbon atoms. Different conditions and values of the parameters have been explored, within certain limits. The most important parameters are: $N_{\rm C}$, $\alpha_{\rm asym}\ E_{\rm ej}^{1/2}$, β, μ and $T_{\rm g}$. We have found a set of parameters giving a rather good fit. This set of parameters and especially the gas and radiation densities, is fully consistent with the observed level of scattered light in the Red Rectangle. The parameters giving this fit are: $\alpha_{\rm asym}\ E_{\rm ej}^{1/2}$ = 0.3 eV$^{1/2}$, $A_{\rm V}$ = 2.0, $T_{\rm g}$ = 35K, μ = 3.0 Debye. Fig. 3 shows this best fit. Although we cannot assert that it is unique, all the other different sets of parameters we have considered have given definitely unacceptable fits (Fig. 4, 5 and 6)

It is important to stress that our model gives a rotational *temperature* , whereas the observational constraints give *bandwiths*. The relationship between the two quantities depends upon the change of the rotational constant, $\Delta B/B$, during the electr. trans.: $\Delta h\nu\ \approx 2.5kT_{\rm rot} \times \Delta B/B$ (see Sect. 6). Scarrott et al. (1992) have considered $\Delta B/B = -3\%$ that gives a good fit to the band profiles and leads to $T_{\rm rot}$ = 450K at 6 arcsec. From molecular physics considerations, this is probably a maximum value for $\Delta B/B$, but smaller values, e.g. $\Delta B/B = -1\%$, give also correct band profiles fits and lead to quite different temperatures, e.g. 1350 K at 6 arcsec. Therefore, considering the Red Rectangle alone cannot yield a molecular size (Fig. 3). The radial dependence of the temperature is actually a more useful criterium for parameters adjustment.

5.1. Rocket effect

The effect of reducing $\alpha_{\rm asym}\ E_{\rm ej}^{1/2}$ from 0.3 (Fig. 3) to 0.03 eV$^{1/2}$ is shown on Fig. 4: no fit can be found for any molecular size. This is also true as long as $\alpha_{\rm asym}\ E_{\rm ej}^{1/2}$ is lower than 0.15 eV$^{1/2}$. A first and important conclusion is that an important rocket effect is mandatory to obtain an acceptable fit of the Red Rectangle data, with high enough temperatures. Of course one cannot disentangle the respective role of the energy of ejection and of the asymmetry. A possible share between the two processes is $E_{\rm ej}$ = 1 eV and $\alpha_{\rm asym}$ = 0.15.

5.2. Role of radio emission

If the molecule has a small dipole moment μ, then the slope of $T_{\rm rot}$ vs θ remains flat, as illustrated on Fig. 5. This is because the other dominant effects (infrared emission and rocket effect) are all linearly dependent either on $n_{\rm H}$ or on $U_{\rm UV}$ which, both, are varying as θ^{-2}, this dependence cancelling then out. We conclude that the radio cooling is needed to obtain an efficient

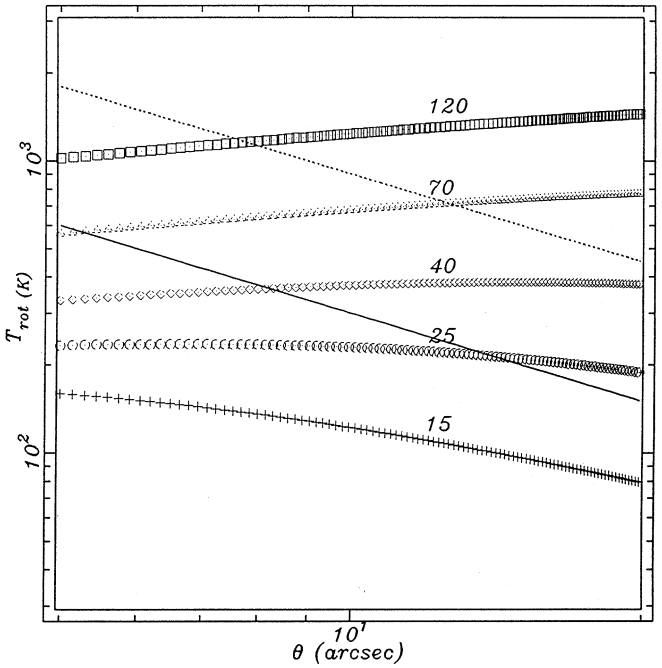

Fig. 5. Same as Fig. 3, but with μ = 1.0 Debye: there is no good fit of the slope wathever the PAH size is.

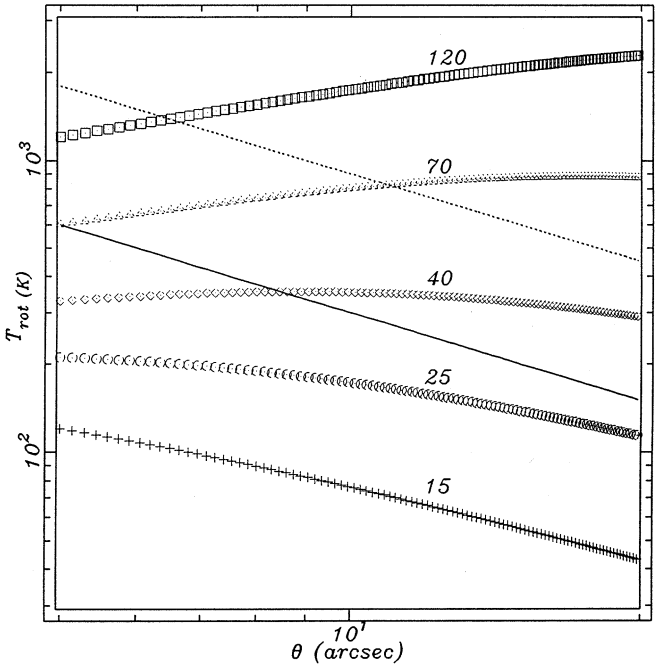

Fig. 6. Same as Fig. 3, but with A_V = 1.4: the IR emission imposes the temperature, which is lower than the observed one; the slope is also very different.

decrease of the rotational temperature with distance. Quantitatively, a dipole moment of $\approx$ 3 Debye is required. There is a certain coherence in the need of a rather large dipole moment and of a high asymmetry factor $\alpha_{\rm asym}$, both properties being probably connected.

5.3. Exchanges with the gas

Despite our result that the kinetic gas temperature is likely below 30 K everywhere in the envelope, we have considered the case of higher values ($T_{\rm gas}$= 100 K at 10 arcsec), varying with the distance to the star according to a $r^{-1.7}$ law, as modelized in the case of IRC10216 (Keady, Hall & Ridgway, 1984; Goldreich & Scoville, 1976). This is shown on Fig. 7. We can check that the decrease of $T_{\rm gas}$ with radius helps for fitting accurately the observed [-1] slope of $T_{\rm rot}$ vs θ, but one can show that this process, alone, is not sufficient and, we repeat it, unlikely.

5.4. Exchanges with the radiation field

The role of the UV field is important, because if the UV intensity is too large, then the IR emission would clamp the temperature to $T_{\rm IR} \approx$ 150 K, as shown in Paper I, and illustrated on Fig. 6 where A_V = 1.4. The opacity of the envelope appears thus as one of the parameters most constraining the model; however it is worth noting that the range of A_V giving an acceptable fit, i.e. $A_V \approx$ 1.7 - 2.3, is within the one that agrees with observational constraints on the scattered light (Sect. 2).

As a conclusion, from the observational constraints on the λ 5797 DIB observed in emission in the Red Rectangle, we cannot deduce a carrier size because of our ignorance of the value for $\Delta B/B$.

6. Rotational temperature in the diffuse ISM and Reflection Nebulae

In order to test our model, we now consider two cases where physical conditions are different enough from the Red Rectangle to lead to predictions by our molecular model that can differ significantly from those in the Red Rectangle.These two cases are the Diffuse Interstellar Medium and a typical Reflection Nebula.

6.1. Case of the ISM

The physical conditions that we consider for the diffuse ISM are the same as in Paper I (Table I), namely:

$$U_{\rm UV} = 0.08\text{eV cm}^{-3}$$
$$n_{\rm H} = 30\ \text{cm}^{-3}$$
$$T_{\rm gas} = 100\ \text{K}$$
$$\beta = 0.1$$

From the most recent observations of the λ 5797 DIB (Ehrenfreund & Foing, 1995; Westerlund & Krelowski, 1988, Sarre et al., 1995), one derives a FWHM of the band of 2.3 cm^{-1}. Because of this small width, we can no longer assume that the broadening is due solely to the asymmetric rotational structure induced by $\Delta B \neq 0$, as already discussed in the beginning (see also Schmidt & Witt 1991), but that the broadening by

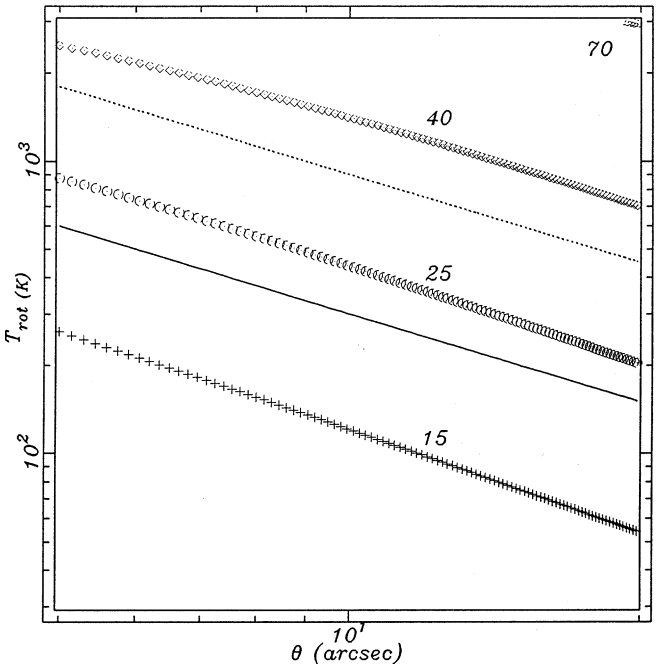

Fig. 7. Same as Fig. 3, but with a gas kinetic temperature higher and varying as $\theta^{-.7}$: the decrease of rotational temperature with radius is only slightly increased.

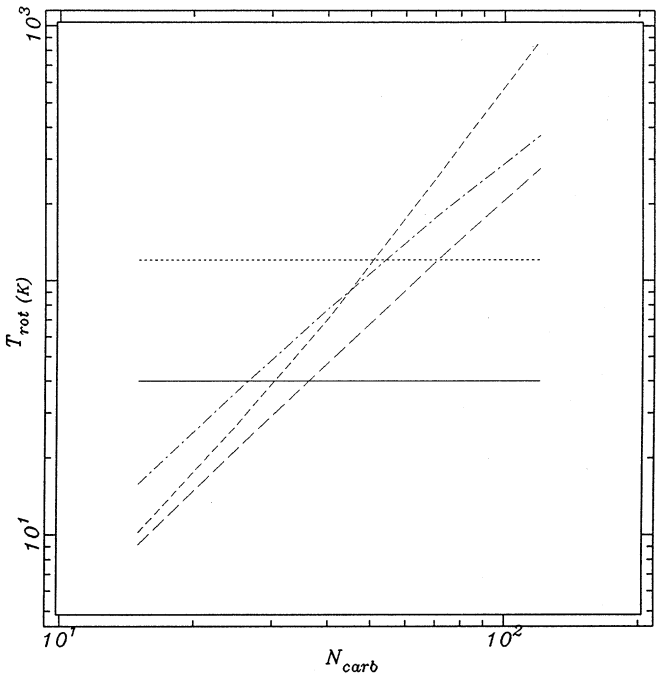

Fig. 8. Computed rotationnal temperature versus the molecule size (in number of carbon atoms) in conditions typical of the *diffuse ISM*. Short-dash: nominal conditions (see text); long-dash: $n_{\rm H}$ = 30 cm^{-3}; dash-dotted: $U_{\rm UV}(\theta)$ = 0.24eV cm^{-3}. The two horizontal lines (solid and dotted) correspond to the rotational temperature deduced from observations when$\Delta B/B$ = 3% and 1% respectively.

the P,Q,R separation (which depends on the temperature) must also contribute. Using a comparison with results published in the literature on theoretical band profiles of various species (Edwards & Leach, 1993; Cossart-Magos & Leach, 1990; Scarrott et al., 1992), and using also an approximation by the linear molecule, which fits remarkably well the cases of benzene and of coronene, we have derived the following empirical relation between temperature and width of the band:
$\Delta(h\nu) = 2.5kT_{\rm rot} \times \Delta B/B + 4(BkT_{\rm rot})^{1/2}$.
Assuming, as previously, $\Delta B/B < 3.\ 10^{-2}$ and $B \propto N_{\rm C}^{-2}$, we can solve this equation for different values of $N_{\rm C}$. The resulting $T_{\rm rot}$ ranges between 18 and 35 K when $N_{\rm C}$ varies from 15 to 30 atoms. Contrary to the case of the Red Rectangle, the rotationnal temperature appears now largely *infra-thermal*.

Taking into account all the processes described in Sect. 4, and the above listed characteristics of the ISM, we can solve Equ.4 for different values of the molecular parameters, and compare the resulting theoretical $T_{\rm rot}$ to the observed one.

We have allowed variation of the molecule size and of the dipole moment within the respective ranges found in the case of the RR; the poorly known dehydrogenation fraction and the UV flux have also been varied. The results are presented on Fig. 8 where the computed rotational temperature is plotted vs the PAH size for three different set of parameters. One can see that, for small PAHs in the range 20 - 30 atoms, there is a good agreement between the predictions of the model and the observations, when using the molecular parameters best fitting the data in the RR. We reach thus the important conclusion that *our model can reproduce with the same set of molecular parameters, the case of the ISM and of the RR, despite the very different physical conditions*.

6.2. Case of Reflection Nebulae

The physical conditions that we consider for the typical Reflection Nebula are the one of NGC2023, i.e. as in Paper I (Table I), namely:

$$U_{\rm UV} = 50.\text{eV cm}^{-3}$$
$$n_{\rm H} = 10^3 \text{ cm}^{-3}$$
$$T_{\rm gas} = 100 \text{ K}$$
$$\beta = 0.98$$

Using those parameters, we compute the rotational temperature for different sizes of PAH. The result is displayed in Fig. 9 for the nominal set of parameters and for two other cases, one where the UV flux is divided by a factor of 3 and one where the gas density is increased by a factor of 3. The most important characteristic is that the predicted temperature remains in all cases close to 100 K and is almost independent of the PAH size. This is a direct illustration of a remark we have made in Paper I: as soon as UV irradiation becomes important, the number of IR photons emitted is large and dominates the exchange of angular momentum with the PAH molecule: the rotational temperature becomes then locked at a temperature of $\approx$ 100 K, almost independently of the size of the molecule. This is an important

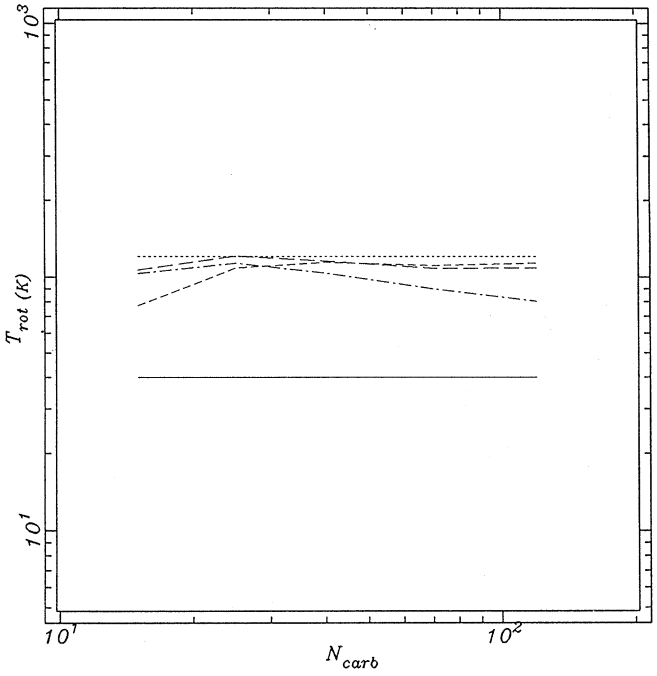

Fig. 9. Computed rotationnal temperature versus the molecule size (in number of carbon atoms) in conditions typical of a reflection nebula. Dash-dotted: nominal (see text); long-dash: $n_{\rm H}$ = 3 10^3 cm^{-3}; short-dash = $U_{\rm UV}(\theta)$ = 15eV cm^{-3}. The two horizontal lines (solid and dotted) correspond to the rotational temperature deduced from observations when$\Delta B/B$ = 3% and 1% respectively.

prediction of our model: in RNs the width of the DIB, when dependent on the rotational temperature, must be in agreement with a typical temperature of 100K. The straightforward consequence of this prediction is that, provided that the conditions of strong illumination are actually met, the width due to the rotational structure must give directly a fair estimate of $\Delta B/B$.

To compare this prediction with observations, we used the data from Josafatsson & Snow (1987) who specifically addressed the question of a possible relation between the DIB band structure and the excitation of the carrier in regions of high radiation field. They observed 37 stars known to be in reflection nebulae with different E(B-V) color excess. We have examined the few cases for which the spectrum was available (Fig. 1 of latter paper) and the extinction not too large, in order to have a good chance that the medium in which the line is formed is also well irradiated by the star, but of course, this may not be actually always the case. It is possible to derive a FWHM for half a dozen of such stars and we find an average width of 1.1 Å with a small dispersion. This value seems significantly higher than the 0.75 Å width observed in the diffuse ISM (Westerlund & Krelowski, 1988), even if one considers the medium spectral resolution (0.4 Å) of those spectra. It is unlikely that this difference be due to Doppler broadening by several clouds on the line of sight, those stars being rather close and clearly associated to the cloud where the extinction takes place; this is confirmed by the fact that the shape of the band looks very much as the one observed in the ISM, especially the red tail. We propose to interpret this larger bandwith, as compared to the ISM, as due to larger rotational temperature in the RNs than in the ISM. Translating this width to $\Delta\sigma$ = 3.3 cm^{-1}, we derive then $\Delta B/B \approx -.02$ a value which is not unrealistic.

If our interpretation is correct, then we have found an almost completely determined solution in terms of *molecule size*, with the following steps of reasoning: *i)* the temperature in the Red Rectangle and the ISM, strongly dependent on the PAH size, constrains a range of size, directly dependent on the range of $\Delta B/B$; *ii)* the rotationnal temperature in RNs, independent on the molecule size, imposes the value of $\Delta B/B$. Now, this observational constraint has an important implication: it removes the degeneracy in the product $\Delta(h\nu) \approx kT_{\rm rot} \times \Delta B/B$. As $kT_{\rm rot}$ is determined in our model, independently from the molecular size, the measurement of $\Delta\lambda$ = 1.1Å, or $\Delta h\nu$ = 3.3 cm^{-1} fixes $\Delta B/B \approx -2\%$.

7. Conclusion

In order to interpret the width of the rotational structure of the λ5797 DIB observed: a) in absorption in the diffuse ISM and Reflection Nebulae; b) in emission in the Red Rectangle, we have explored a model that assumes that the carrier of the DIB is a free PAH molecule, and we have calculated its rotational temperature. We stress that the derivation of a temperature from the width of the band depends essentially on the value of $\Delta B/B$, the relative variation of the rotational constant between the two levels of the electronic transition, a parameter which is unknown but whose modulus should be less than 3%, when compared to other molecular species.

One of the strongest observational constraint comes from the high rotational temperature in the Red Rectangle ($T_{\rm rot} > 450K$ at θ= 6 arcsec), and its dependence with radial distance to the star ($T_{\rm rot} \propto r^{-1}$). Firstly, we have shown that, *if* there is no gas heating mechanisms other than grain collisions and photo-electric effect, the gas temperature is *much too low* to explain the implied molecule rotational temperature. In a second step, a self-consistent model of the gas density and radiation structure in the Red Rectangle is derived from observational constraints, mainly based on scattered light intensity data; this model has then been used to compute the rotational temperature and its radial dependence, taking into account all the processes exchanging angular momentum with a PAH. A reasonable range for each parameter has then been explored, leading to several conclusions:

a) We show that a very efficient *rocket effect* based on the ejection of H atoms or molecules from peculiar sites of the molecule, is needed to get the observed supra thermal rotation in the RR. If one cannot disentangle the respective roles of the asymmetry and of the energy of ejection, however, one can quote as typical values: $E_{\rm ej}$ = 0.3eV and $\alpha_{\rm asym}$ = 0.3, a set which is consistent, for instance, with the ejection of a H_2 molecule just after it forms on a peculiar site of the PAH, using a fraction of the formation energy.

b) Among all the invoked physical processes, the emission of radio photons is needed to explain the decrease as r^{-1} of the

temperature, constraining the size of the carrier of the DIB to be a rather small molecule that would feature typically *20 to 50 atoms*, for a reasonable range of $\Delta B/B$. All the other processes considered lead to a flat behaviour of the temperature with distance. A dipole moment of several Debye is needed in order to obtain a clear decrease of $T_{\rm rot}$ with radial distance.

c) It is pointed out that only a rather narrow range for each parameter can be found to obtain a satisfactory fit to the observational data, generally much less than one order of magnitude: in other words, the acceptable volume in the phase space of parameters is a narrow one, but for $\Delta B/B$ and consequently N_c, when the Red Rectangle alone is accounted for.

It is not clear, however, if this last result should be considered as a support of our model – this may explain for instance why the Red Rectangle is a very unique object [2] – or as an argument against it because the model may appear as an *ad hoc* one. This is why, in order to check the consistency with other observations in the Interstellar Medium, we have, in a second step, used the molecular parameters (size, asymmetry, dipolar moment, etc.) found for our "best DIB carrier" in the Red Rectangle, to compute the rotational temperature, that would fit DIB in absorption, in the ISM, and typical Reflection Nebulae, where the physical conditions are quite different from those in the Red Rectangle. In the former case, we find a good fit between the prediction of the model and the observed rotational temperature of the interstellar DIB, especially if we take into account the fact that a large variation of physical conditions along the line of sight may affect the comparison with the model. Moreover, we show that varying largely the physical conditions of the environment (gas and radiation density) does not change significantly the rotational temperature: we argue that this would explain the well known fact that the observed width of DIBs is essentially constant in all directions in the galactic plane, but for Doppler broadening (e.g. Herbig & Leka, 1991). In the case of the Reflection Nebulae, our model predicts that the PAH *temperature must be locked* onto a value of the order of 100 K – essentially set by the emission of IR photons that dominates the angular momentum exchange –, practically independently from the PAH size. Indeed we note that the width of the λ 5797 DIB observed in stars illuminating Reflection Nebulae appears significantly broader, typically by 40%, than in the diffuse ISM and we interpret this by an actual difference in the rotational temperatures reached in those two different environments. This interpretation then *removes the underdetermination of* $\Delta B/B$ and leads to a value $\approx$ - 2%, for this carrier, and, in turn, to a derivation of the size of the λ 5797 DIB carrier: $\approx$ 40 carbons, a molecule somewhat larger that ovalene.

We feel that the consistency of predictions by our model for so different environments as those found in the ISM, Reflection Nebulae and in the RR, can be considered as a support of our proposal that a free PAH, with typically *40 atoms*, is the carrier of this DIB; anyhow, the very precise characteristics of the proposed carrier *lead to observational predictions*, for instance on the measurement of DIBs in Reflection Nebulae with a high signal to noise ratio, that will allow a check of our model.

[2] We have searched, without success, up to now, for DIBs in emission in several reflection nebulae

8. Annex A

Equ. 4 can be written as:

$$\begin{aligned} y(J) &= a_{\rm radio}J^4 + (b_{\rm IR} + b_{\rm friction})J^2 \\ &\quad -c_{\rm rocket}J - (d_{\rm IR} + d_{\rm coll}) \\ &= 0 \end{aligned}$$

where all quantities ($a_{\rm radio}, b_{\rm IR}, b_{\rm friction}, c_{\rm rocket}, d_{\rm IR}$ and $d_{\rm coll}$) are positive. Taking the derivative of $y(J)$ and looking for the roots, leads to a third order polynomial equation that can be solved exactly. Because the coefficients of J^4 and of J^2 are of the same sign, one can show that only one solution of this equation is real: there is then only one extremum of $y(J)$. On the other hand we can check that $y(0)$ is negative, because $d_{\rm IR} + d_{\rm coll}$ is positive, and $y(J \rightarrow \pm\infty)$ is positive: this means that $y(J)$ must cut the J axis at two points which are the two real roots of $y(J) = 0$. Finally, we know that in a polynomial equation, the coefficient of J^0, here $-(d_{\rm IR} + d_{\rm coll})$, is the product of all the roots times $(-1)^{N_{\rm root}}$; here $y(J)$ having 4 roots and two of them being conjugate complex, i.e. their product being positive, we conclude that the two real roots are of opposite sign: only one root is positive and thus has a physical meaning in the problem we are dealing with.

Acknowledgements. We thank P. Thaddeus for a fruitful discussion during the 1994 workshop at Boulder ("The diffuse Interstellar Bands"), and the referee, A. Witt, who has helped clarifying the paper.

References

Cohen M., et al. 1975, ApJ 196, 179
Cossart-Magos C., Leach S., 1990, A&A 233, 559
Crawford M.K., Tielens A.G.G.M., Allamandola L.J., 1985, ApJ 293, L45
Draine B.T., Lee H.M. 1984, ApJ 285, 89
Edwards S.A., Leach S., 1993, A&A 272, 533
Ehrenfreund P., Foing B.H., 1996, A&A 307, L25
Goldreich P., Scoville N.Z., 1976, ApJ 205, 144
d'Hendecourt L.B., Léger A., 1987, A&A 180, L9
Herbig G.H., Leka K.D., 1991, ApJ 382, 193
Herzberg G., 1968 a,b, Diatomic molecules (a), Infrared and Raman Spectra of Polyatomic Molecules (b). vanNostrand
Joblin C., Léger A., Martin P., 1992, ApJ 393, L79
Josafatsson K., Snow T.P., 1987, ApJ 319, 436
Keady J.J., Hall D.N.B., Ridgway S.T., 1988, ApJ 326, 832
Kurucz R.L. 1979, ApJ 40, 1
Léger A., d'Hendecourt L., 1985, A&A 146, 81
Léger A., d'Hendecourt L., Défourneau D., 1989b: A&A 216, 148
Lopez B., Mékarnia D., Lefèvre J., 1995, A&A 296, 752
McClelland G.M., Nathanson G.M., Frederick J.H. Farley F.W., 1988, Excited states, vol. 7, p. 83, Academic Press
Purcell E.M., 1969, Physica 41, 100
Purcell E.M., 1979, ApJ 231, 404
Roddier F., Roddier C., Graves J.E., Northcott M.J., 1995, ApJ 443, 249

Rouan D., Léger A., Omont A., Giard M., 1992, A&A 253, 498
Rouan D., Léger A., 1995, in The Diffuse Interstellar Bands, 165, A.G.G.M. Tielens, T.P. Snow (eds), Kluwer Academic Publishers.
Rouan D., Lecoupanec P., Léger A., 1995 in 1st Franco-British Conference on the Physics and Chemistry of the Interstellar Medium Lille, July 10-12 /1995
Sarre P.J. et al., 1995, MNRAS 277, L41
Sarre P.J., Miles J.R., Scarrott S.M., 1995, Science 269, 674
Scarrott S.M., Watkin S., Miles J.R., Sarre P.J., 1992, MNRAS 255, 11P
Schmidt G.R., Cohen M., Margon B., 1980, ApJ 239, L133
Schmidt G.D., Witt A.N., 1991, ApJ 383, 698
Spitzer L., 1978, Physical Processes in the Interstellar Medium. Wiley, Sons
Tessier E., Perrier C., Léna P., Michel G., Langlet A., 1990, in Astrophysics with infrared arrays, ed. R. Elston, ASP Conf. ser. 14, p. 145
Townes C.H., Schawlow A.L., 1975, Microwave Spectroscopy. Dover, New York
Van der Zwet G.P., Allamandola L.J., 1985, A&A 146, 76
Van Winckel H., Waelkens C., Waters L.B.F.M., 1995, A&A 293, L25
Waelkens C., Van Winckel H., Trams N.R., Waters L.B.F.M., 1992, A&A 256, L15
Waelkens C., Van Winckel H., Waters L.B.F.M., Bakker E.J., 1996, A&A 314, L17
Warren-Smith R.F., Scarrott S.M., Murdin P. 1981, Nature 292, 317
Westerlund B.E., Krelowski J., 1988, A&A 203, 134
Yuseph-Zadeh F., Morris M., White R.L., 1984, ApJ 278, 186

This article was processed by the author using Springer-Verlag LaTeX A&A style file *L-AA* version 3.